Int. J. Electrochem. Sci., 8 **(2013)** 6678 - 6685

International Journal of
ELECTROCHEMICAL
SCIENCE
www.electrochemsci.org

Plasma-Enhanced Storage Capability of SONOS Flash Memory

Chi-Chang Wu[1,], Wen-Luh Yang[2], Yuan-Ming Chang[2,3], Sheng-Hsien Liu[2,3], Yu-Ping Hsiao[2,3]*

[1] Graduate Institute of Biomedical Materials and Tissue Engineering, College of Oral Medicine, Taipei Medical University, Taipei, Taiwan
[2] Department of Electronic Engineering, Feng Chia University, Taichung, Taiwan
[3] Ph.D. Program in Electrical and Communications Engineering, Feng Chia University, Taichung, Taiwan
[*]E-mail: halfccwu@tmu.edu.tw

Received: 2 April 2013 / *Accepted:* 15 April 2013 / *Published:* 1 May 2013

High-κ thin film is a candidate material for the charge storage layer of non-volatile flash memory. This material can achieve faster programming speeds and better charge-retention performance. This paper reports the fabrication of a $Co_xHf_ySi_zO$ high-κ thin film formed by using a sol-gel technique and low-temperature annealing. The proposed fabrication method involves using oxygen plasma treatment to passivate the surface of the high-κ film and maintain low-temperature formation with high quality. The X-ray analysis presented in this study showed that the $Co_xHf_ySi_zO$ high-κ film formed metal-rich cobalt and hafnium silicate after oxygen plasma treatment, thus improving the performance of the $Co_xHf_ySi_zO$ high-κ memory by creating more trapping sites. This plasma treatment also improves the memory window from 1.92 to 2.16 V. The retention can decrease to 13% at a 10^6 s measurement, and the memory narrowing for the plasma-treated $Co_xHf_ySi_zO$ high-κ memory is 21% after 10^6 program and erase cycles. The sol-gel method resulting $Co_xHf_ySi_zO$ high-κ flash memories show that oxygen plasma treatment improves the memory performance in retention and endurance.

Keywords: SONOS, flash memory, plasma treatment, sol-gel

1. INTRODUCTION

Flash memory devices have generated increased interest in portable electronic products because of their high data retention, low cost, and low power consumption characteristics [1]. Conventional flash memory devices use a floating gate (FG) structure that stores charges in a poly-silicon floating gate [2, 3]. However, as conventional FG memory devices continue to shrink, they often suffer from a charge loss problem [4]. The stored charges leak because of defects in the tunneling oxide formed by

repeated program and erase cycles. Therefore, many researchers have studied thin film poly-Si-oxide-nitride-oxide-silicon (SONOS) memories to replace the floating gate structure in semiconductor memory applications [5]. High-κ thin films have recently been used as charge storage materials, enabling faster programming speed and better charge retention performance [6]. High-κ film is expected to preserve trapped charges more efficiently, and demonstrates excellent features such as low programming potentials and high programming and erasing speeds. Hence, high-κ film can significantly improve memory performance [7].

This study presents a relatively simple and inexpensive technique for forming high-κ thin film. Specifically, the sol–gel spin-coating method and post-annealing were used to form metal-oxidized high-κ thin film [8]. The sol-gel film was transformed into a solid thin film after undergoing thermal annealing in an O_2 ambient. The spin-coating method is much simpler than other film fabrication methods because of its easy operation, relatively cheap precursor, and lower tool price [9-11]. The resulting film can be fabricated in an atmospheric pressure system instead of a complex, high-vacuum system [12]. However, previous studies have shown that high-temperature post-annealing is required to obtain a satisfactory high-κ film [13, 14]. This high-temperature post-annealing, which is usually above 900 °C, hinders the wide application of the sol-gel method for thin film transistors or flexible devices.

This paper presents a $Co_xHf_ySi_zO$ high-κ thin film formed using the sol-gel method with post-annealing at 500 °C. An oxygen plasma treatment was used after annealing to achieve low-temperature formation with high quality. This plasma process is often used in integrated circuit fabrication. This study investigated the effects of O_2 plasma treatment on the electrical properties of high-κ memory, and evaluated the memory window, retention, and endurance to assess overall performance.

2. MATERIALS AND METHODS

The fabrication of high-κ memory began with a local-oxidation of silicon (LOCOS) isolation on a 6-in, p-type (100) silicon wafer. A tunnel oxide layer measuring 6 nm thick was thermally grown at 925 °C by performing furnace oxidation. A charge trapping layer was then prepared using a sol-gel spin coating method. The precursors used for the preparation of the sol-gel solution were analytical reagent grade cobalt dichloride ($CoCl_2$-$6H_2O$, 99.5%, Aldrich), hafnium tetrachloride ($HfCl_4$, 99.5%, Aldrich), and silicon tetrachloride ($SiCl_4$, 99.5%, Aldrich). Ethanol (EtOH) solvent was used to dissolve the precursors in preparing the sol-gel solution. Hydrochloric acid was added to the solution to catalyze the gels into small ultimate particles. The solution was stirred for 0.5 h after preparation to ensure complete mixing. A sol-gel solution with a 1:1:1:1000 molar ratio of $CoCl_2$-$6H_2O$: $HfCl_4$: $SiCl_4$: EtOH was prepared. This solution was spin-coated on the substrate at a rotation speed of 3000 rpm for 60 s at room temperature. Rapid thermal annealing (RTA) was then performed at 500 °C for 60 s in an O_2 ambient, followed by an oxygen plasma treatment for 20 s in a vacuum chamber. The temperature and power of the plasma treatment were maintained at 300 °C and 150 W, respectively.

After the high-κ thin film was formed, a 20-nm-thick blocking oxide was deposited immediately by using plasma enhanced chemical vapor deposition (PECVD) with tetraethoxysilane

(TEOS) oxide. A 200-nm amorphous Si layer was then deposited to form the gate electrode. Finally, the gate pattering, source/drain (S/D) implanting, and the remaining subsequent metal-oxide-semiconductor (MOS) processes were used to fabricate the $Co_xHf_ySi_zO$ high-κ flash memory. Fig. 1 shows a schematic diagram of the high-κ memory structure.

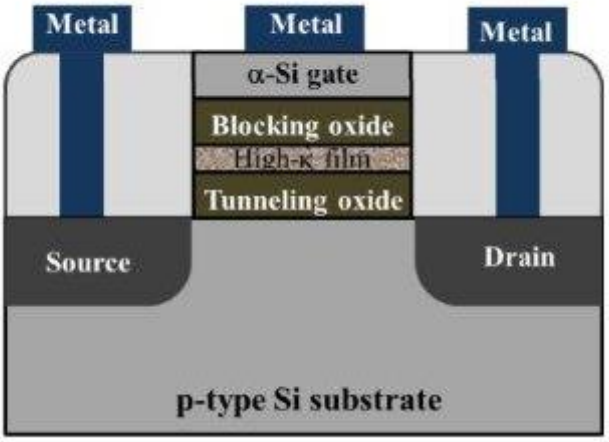

Figure 1. Schematic diagram of high-κ flash memory.

The microstructure of the high-κ thin film was examined using transmission electron microscopy (TEM). The chemical composition of the film was verified using energy dispersive spectroscopy (EDS) and X-ray photoelectron spectroscopy (XPS). The electrical characteristics of the high-κ memories were determined using an Agilent 4156 semiconductor parameter analyzer. The feather sizes of the measured devices reported in this paper had a channel width and length of 10 μm and 0.35 μm, respectively.

3. RESULTS AND DISCUSSION

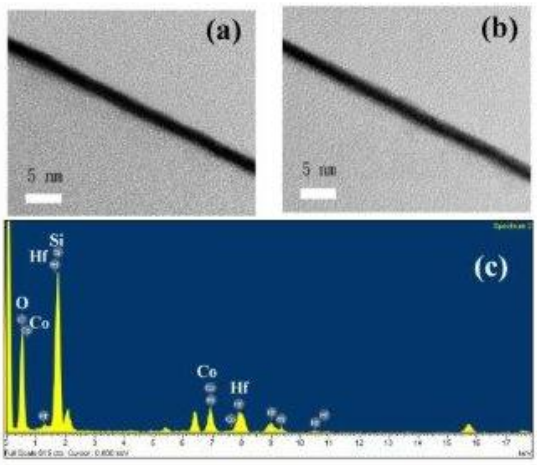

Figure 2. Cross-sectional TEM images of $Co_xHf_ySi_zO$ high-κ thin film (a) before and (b) after O_2 plasma treatment. (c) EDS spectrum of the plasma treated $Co_xHf_ySi_zO$ high-κ thin film.

Figs. 2(a) and 2(b) show a comparison of the cross-sectional TEM images of the $Co_xHf_ySi_zO$ high-κ thin film before and after O_2 plasma treatment. These figures clearly show that the high-κ thin films are smooth before and after plasma treatment. The thickness of the high-κ thin film was maintained at approximately 3 nm, even after plasma treatment. Fig. 2(c) shows the EDS spectrum of the high-κ thin film, indicating that the film consists of $Co_xHf_ySi_zO$ material.

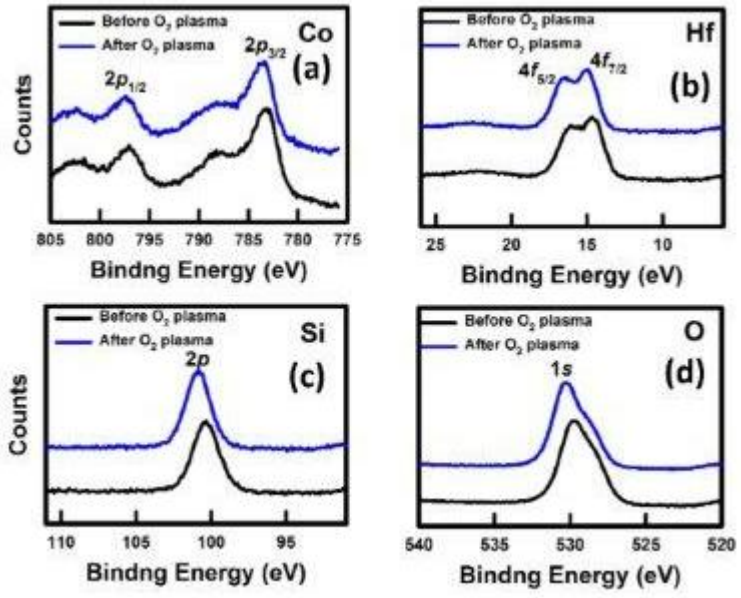

Figure 3. (a) Co 2*p*, (b) Hf 4*f*, (c) Si 2*p*, and (d) O 1*s* spectra of the sol-gel derived $Co_xHf_ySi_zO$ high-κ film before and after O_2 plasma treatment.

Fig. 3 presents a comparison of the XPS results for (a) Co 2*p*, (b) Hf 4*f*, (c) Si 2*p*, and (d) O 1*s* bonding for samples before and after O_2 plasma treatment. The binding energies of Co 2*p* and Hf 4*f* exhibit a slight shift to higher energies after plasma treatment. Fig. 3(c) shows an increase in the binding energy of Si 2*p* from 100.35 to 100.65 eV after O_2 plasma treatment. This result relates to the oxidization of Si toward the blue-shift [15]. For the O 1*s* spectra in Fig. 3(d), each peak can be deconvoluted into two peaks (i.e., the higher- and lower-energy peaks), which respectively represent the Si-O and metal-rich silicate [16]. The intensity ratio of the lower-to-higher energy peak increases after O_2 plasma treatment. This observation suggests that the Co–O and Hf–O reacts with nearby Si atoms, forming cobalt and hafnium silicate. Because the metal-rich silicate creates deeper trapping sites than the oxide-rich silicate does, the electrical performance of the $Co_xHf_ySi_zO$ high-κ memory should improve after oxygen plasma treatment. Fig. 4 shows a comparison of the I_d-V_g curves of the sol-gel derived $Co_xHf_ySi_zO$ memories with and without O_2 plasma treatment in program and erase states. Channel hot-electron injection (CHEI) was used to program the flash memory devices, and band-to-band hot-hole (BBHH) injection was used to erase charges [17]. The applied program voltages were V_g = 9 V and V_d = 9 V, and the erase voltages were V_g = -8 V and V_d = 8 V, with 10 ms of operation time. The memory windows, which represent the threshold voltage (V_{th}) difference between the program and erase states, were estimated to be 1.92 V and 2.16 V for the memories with and without O_2 plasma treatment, respectively. The memory window widened after O_2 plasma treatment. This is likely because of the formation of metal-rich silicate, which created more trapping sites in the

$Co_xHf_ySi_zO$ high-κ film [18]. The I_d-V_g curve of the memory in the erase state can be completely recovered to the original fresh state without any distortion. This result is essential for memory devices that require greater stability and better data retention characteristics.

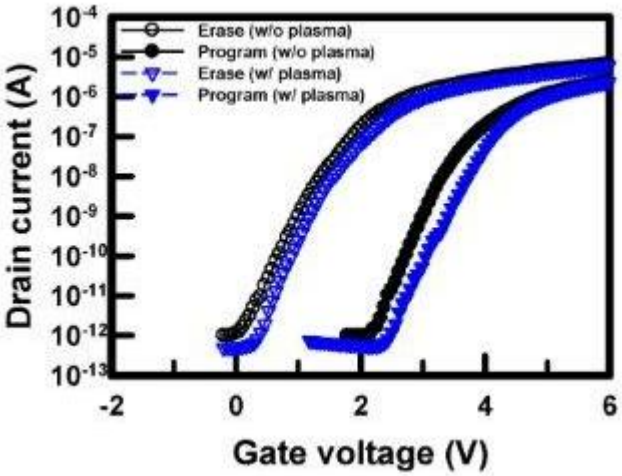

Figure 4. I_d-V_g characteristics of the high-κ memories with and without O_2 plasma treatment in fresh and program states, respectively.

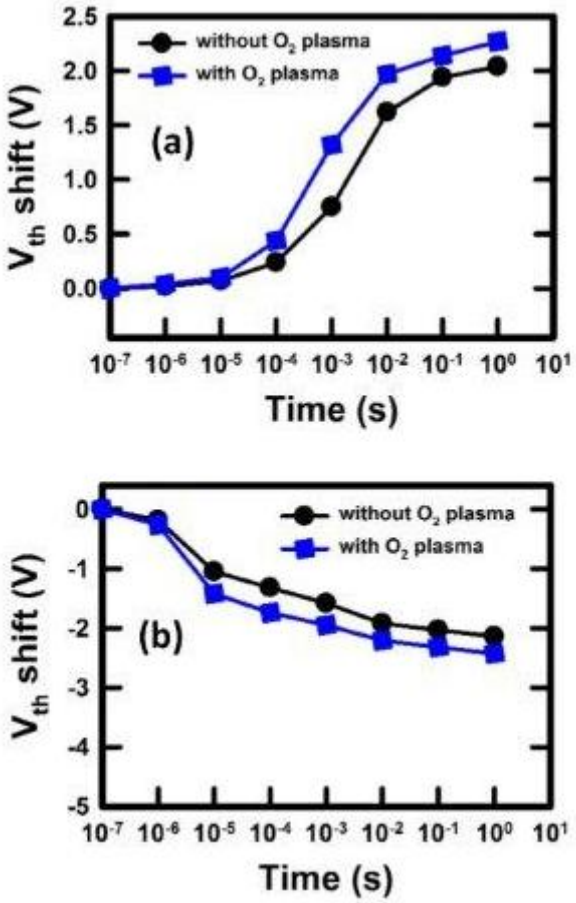

Figure 5. (a) Program and (b) erase speeds of the $Co_xHf_ySi_zO$ high-κ memories.

Figs. 5(a) and 5(b) show the program and erase speeds of the $Co_xHf_ySi_zO$ high-κ memories with and without O_2 plasma, respectively. The program condition used here was $V_d = V_g = 9$ V. The V_{th} shift increases with the programming time because more hot electrons are injected through the tunnel oxide and are trapped in the trapping sites of high-κ thin film. The V_{th} shift can be as much as 2.3 V after 1 s of programming for a sample undergoing O_2 plasma treatment, whereas only 2 V is available for a sample without O_2 plasma. The program speed is 15 ms with a 2 V V_{th} shift for a sample undergoing plasma treatment, whereas a sample without O_2 plasma requires 293 ms. The characteristic of fast program speed originates from the additional trapping sites provided by the Co and Hf silicates of high-κ thin film after O_2 plasma treatment. Thus, electrons can be trapped rapidly and smoothly in the memory. The erase condition by BBHH method was $V_d = 8$ and $V_g = -8$ V. The same result of program speed measurement is observed: the V_{th} shift reaches 2.4 V for the sample after plasma treatment, but only 2.1 V for the sample without O_2 plasma treatment.

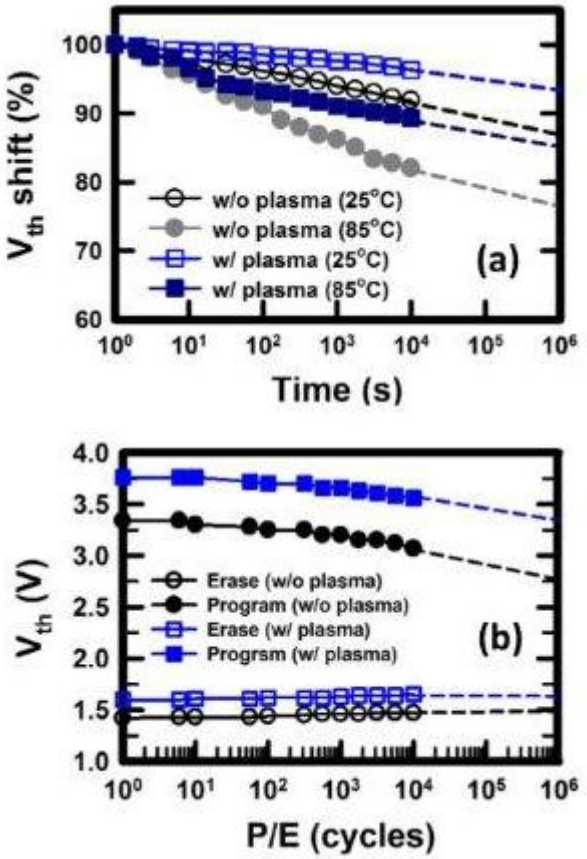

Figure 6. (a) Charge retention and (b) endurance characteristics of the high-κ memories with and without O_2 plasma treatment.

To inspect the reliability concerns of the high-κ memory, this study compared the retention and endurance characteristics. Fig. 6(a) shows the charge retention characteristics of the $Co_xHf_ySi_zO$ high-κ memories measured at 25 °C and 85 °C. For the sample without O_2 plasma treatment, the retention time can be extrapolated up to 10^6 s for a 13% or 24% charge loss at a 25 °C and 85 °C measurement, respectively. Plasma treatment significantly improved the charge loss to 7% and 15% under the same operating conditions. The electron-trapping ability of the $Co_xHf_ySi_zO$ high-κ memory was much higher

after O_2 plasma treatment. Fig. 6(b) shows the endurance of high-κ memories extrapolated up to 10^6 programming and erasing (P/E) cycles. The window narrowing of the memories after 10^6 P/E cycles were estimated to be 34% and 21% for the samples with and without O_2 plasma treatment, respectively. The shifts of threshold voltages in the program and erase states were much improved after a couple of P/E cycles for samples with O_2 plasma treatment. The electrical results of retention and endurance indicate that O_2 plasma treatment enhances the reliability characteristic of the proposed sol-gel-derived and low-temperature-formed $Co_xHf_ySi_zO$ high-κ thin film memory.

4. CONCLUSION

This paper presents a $Co_xHf_ySi_zO$ high-κ thin film as the charge trapping layer of flash memory by using a low-temperature, sol-gel method with a post-O_2 plasma treatment. The TEM and EDS analysis in this study verified the formation of $Co_xHf_ySi_zO$ thin film. The changes in chemical composition were also confirmed using XPS analysis. This study presents a comparison of the electrical characteristics of memories such as memory window, program and erase speeds, and reliability for memory devices with and without O_2 plasma treatment. The results of this study show that post-O_2 plasma treatment can improves the performance of sol-gel-derived $Co_xHf_ySi_zO$ high-κ memory.

ACKNOWLEDGEMENTS
The authors would like to thank Taipei Medical University Hospital and Taipei Medical University, Taiwan, for financially supporting this research under contract no. of 101TMU-TMUH-07.

References

1. S. Maikap, A. Das, T.-Y. Wang, T.-C. Tien, and L.-B. Chang, *J. Electrochem. Soc.*, 156 (2009) K28.
2. N. Chan, M. F. Beug, R. Knoefler, T. Mueller, T. Melde, M. Ackermann,S. Riedel, M. Specht, C. Ludwig, and A. T. Tilke, in Proc. 9th NVMTS, (2008) 82.
3. C.-C. Wu, F.-H. Ko, W.-L. Yang, H.-C. You, F.-K. Liu, C.-C. Yeh, P.-L. Liu, C.-K. Tung, and C.-H. Cheng, *IEEE Electron Dev. Lett.*, 31 (2010) 746.
4. Y.-H. Lin, Y.-C. Wu, M.-F. Hung, and J.-H. Chen, *Int. J. Electrochem. Sci.*, 7 (2012) 8648.
5. B.-Y. Tsui, C.-C. Yen, P.-H. Li, and J.-Y. Lai, *IEEE Electron Dev. Lett.*, 32 (2011) 614.
6. R. Balachandran1, B. H. Ong, H. Y. Wong, K. B. Tan, and M. M. Rasat, *Int. J. Electrochem. Sci.*, 7 (2012) 11895.
7. Y.-H. Lin, H.-C. You, and C.-H. Chien, *J. Vac. Sci. Technol.*, B 30 (2012) 011201.
8. H.-C. You, F.-H. Ko, and T.-F. Lei, *J. Electrochem. Soc.*, 153 (2006) F94.
9. C.-C. Wu, Y.-J. Tsai, P.-L. Liu, W.-L. Yang, and F.-H. Ko, *J. Mater. Sci.: Mater. Electron.*, 24 (2013) 423.
10. J. Katić, M. Metikoš-Huković, R. Babić, and M. Marciuš, *Int. J. Electrochem. Sci.*, 8 (2013) 1394.
11. W.-Y. Su and S.-H. Cheng, *Int. J. Electrochem. Sci.*, 7 (2012) 9058.
12. M.-C. Chu, H.-C. You, J. S. Meena, S.-H. Shieh, C.-Y. Shao, F.-C. Chang, F.-H. Ko, *Int. J. Electrochem. Sci.*, 7 (2012) 5977.

13. F.-H. Ko, H.-C. You, and T.-F. Lei, *Appl. Phys. Lett.*, 89 (2006) 252111.
14. C.-C. Wu, Y.-J. Tsai, M.-C. Chu, S.-M. Yang, F.-H. Ko, P.-L. Liu, W.-L. Yang, and H.-C. You, *Appl. Phys. Lett.*, 92 (2008) 123111.
15. T.-M. Pan and W.-H. Shu, *Appl. Phys. Lett.*, 91 (2007) 172904.
16. W.-R. Chen, T.-C. Chang, P.-T. Liu, J.-L. Yeh, C.-H. Tu, J.-C. Lou, C.-F. Yeh, and C.-Y. Chang, *Appl. Phys. Lett.*, 91 (2007) 082103.
17. H.-C. You, C.-C. Wu, F.-H. Ko, T.-F. Lei, and W.-L. Yang, *J. Vac. Sci. Technol.*, B 25 (2007) 2568.
18. S.-H. Liu, W.-L. Yang, C.-C. Wu, and T.-S. Chao, *IEEE Electron Dev. Lett.*, 33 (2012) 1393.

© 2013 by ESG (www.electrochemsci.org)